Multipath Propagation Analysis of 5G Systems at Higher Frequencies in Courtyard (Small Cell) Environment

Muhammed Usman Sheikh, Joonas Säe, and Jukka Lempiäinen
Laboratory of Electronics and Communications Engineering
Tampere University of Technology (TUT)
Tampere, Finland
{muhammad.sheikh, joonas.sae, jukka.lempiainen}@tut.fi

***Abstract*—The main target of this paper is to study the propagation characteristics of an outdoor and indoor user utilizing 5G system at higher frequency in a courtyard surrounded by building walls i.e. small cell environment. This research work is carried out by doing 3D ray tracing simulations utilizing "sAGA" – a 3D ray tracing tool. Unlike the conventional cellular network frequencies, the considered frequencies in the scope of this work are 15 GHz, 28 GHz and 60 GHz. For simulation routes, the results are provided in the form of received signal strength. For static points, the results are presented in the form of power angular spectrum and power delay profile. The achieved simulation results show that an adequate outdoor and indoor service can be provisioned at the considered frequencies. However, it is challenging to provide services to indoor user at 60 GHz using an outdoor base station even in such a small cell environment.**

***Index Terms*—5G, multipath propagation; small cell; 3D ray tracing, system performance, millimeter wave frequencies**

I. INTRODUCTION

Currently, fifth generation (5G) mobile networks is under a standardization process, and it is set to be delivered by the second half of 2017 as the first set of 5G standards with 3GPP Release 15 [1]. Moreover, 5G is actively discussed in both the industry and academia [2-4]. The discussion about 5G revolves e.g. around utilizing massive multiple-input multiple-output (MMIMO) techniques, new air-interface and radio access network (RAN) systems, and ultra-dense networks. Moreover, it is strongly believed that higher capacity requirements are met with larger frequency bandwidths. However, frequency bands below 4 GHz, which are currently utilized for mobile networks, are already overloaded with existing mobile network technologies. Therefore, the focus has now been on higher frequency bands, called centimeter and millimeter frequencies, i.e. super high frequency (SHF) band ranging from 3 GHz to 30 GHz and extremely high frequency (EHF) band ranging from 30 GHz to 300 GHz, according to the International Telecommunication Union (ITU).

A special interest is given to millimeter wave (mmWave) communication due to large amount of free spectrum available. The problem, however, with utilizing mmWave frequencies and other higher frequencies is increased path loss [5]. When using an isotropic antenna as the transmitter and a fixed size antenna for corresponding frequency in the receiver side, the received power e.g. between 3 GHz and 30 GHz is 20 dB lower for the higher frequency as stated in [6]. Since the antenna apertures sizes are proportional to the used frequency wavelength, the aperture size difference for 3 GHz and 30 GHz signals is tenfold. However, if the aperture size would be fixed and e.g. the whole area of the 3 GHz receiver antenna would be used as an antenna array for 30 GHz, then the received power difference would be zero [6]. Now, if also at the transmitter side the isotropic antenna would be replaced with an antenna array then actually the received power difference is 20 dB larger for the higher frequency due to more directive antennas [6]. Hence, with antenna arrays on both sides, i.e. on the transmitter and receiver side, the higher frequencies have better path loss when excluding any additional losses from atmosphere and weather. Therefore, various R&D organizations are heavily investigating the utilization of higher frequency bands to be utilized in mobile networks [7]. The most interesting and studied frequency bands are those of 15 GHz, 28 GHz, 38 GHz, 60 GHz and 70 GHz [5, 8-11].

In order to properly design a new radio network system, it is important to understand the radio propagation characteristics. The classical propagation prediction models lack the insight information about channel conditions, i.e. the environment, which has to be specified separately. However, deterministic ray tracing models include this information, i.e. they are able to provide the characteristics of radio propagation in a multidimensional environment [12]. Moreover, as a radio signal propagates, it can have different propagation mechanisms, e.g. diffraction from sharp edges (e.g. building corners and rooftops), reflections from smooth surfaces (e.g. ground, walls), transmission into different mediums (e.g. walls), and scattering from rough surfaces or small objects. Therefore, multipath propagation is a complex phenomenon; however, ray tracing is a promising technique to find possible paths between the transmitter and receiver.

The target of this paper is to analyze the multipath propagation characteristics of a courtyard environment for 5G systems. A real world courtyard environment from Yokusuka,

Japan is the basis for the ray tracing simulations as the field measurement results from that area exists in [11]. This paper extends the work done in reference [11] to 28 GHz and 60 GHz frequency bands. A 3D ray tracing tool called "sAGA" is utilized for this study purpose. The simulation tool utilizes image theory (IT) algorithms and is capable of providing several radio propagation properties. The simulation results presented in this paper are utilized to analyze the characteristics of multipath propagation of higher frequency in a courtyard environment.

II. System Model and Environment

A. System Configuration

The simulations performed in this paper are based on the 5G system configuration considered in [11]. The measurement results provided in [11] are limited to only 15 GHz frequency; however the study of this paper also includes 28 GHz and 60 GHz. The utilized 5G system consists of combining four contiguous 100 MHz bandwidth component carriers (CCs) with the help of carrier aggregation (CA) to have a wide 400 MHz bandwidth. The transmission power per CC is set to 27.3 dBm, i.e. the total power of the 4 CC configuration equals 33.32 dBm. The base station is installed with a directional antenna mounted on the wall in the courtyard at 4 m height, with a small tilt angle of 2.3°. The horizontal half-power beamwidth (HPBW) of the directional antenna is 90° and the vertical HPBW is 10.5°. The maximum base station antenna gain is 14.5 dBi. The mobile station has an omnidirectional antenna with 0 dBi gain. The rest of the system configuration is the same as in [11].

B. Simulation Platform

Simulations are performed by utilizing a MATLAB based 3D ray tracing tool called sAGA. The tool is indigenously developed by the authors of the paper. Unlike other quasi-3D ray tracing tools, sAGA performs full three-dimensional ray tracing. Therefore, it is able to find all possible paths between a transmitter and receiver in full three-dimensional environment [13]. In case of reflected paths, the loss in energy due to (specular) reflection is given by the reflection co-efficient. It depends upon the incident and the reflected angle of path as well as material permittivity. The diffraction loss for the diffracted paths is given by Berg's recursive model [14]. In case of scattering, the energy is scattered in a wide range of directions. Furthermore, the impact of scattering becomes significant in higher frequencies. Therefore, a concentric circle approach given at [15] is utilized to generate scattering points on the walls of buildings. For indoor users, the building penetration loss is calculated using the building penetration model given in [16]. Old building type is assumed having 70% concrete and 30% of the windows with double glass. Additional indoor loss is computed using an indoor wall loss model provided at [16].

The sAGA simulation tool provides different characteristics of multipath propagation and provides the results in the form of basic key performance indicators (KPIs) such as received signal strength and signal-to-noise-and-interference ratio (SINR). Other properties like the power angular spectrum (PAS) and the power delay profile (PDP) can be extracted by doing the post processing of 3D ray tracing data. In order to acquire accurate results, ray tracing needs detailed information about the simulation environment. Three-dimensional ray tracing requires 3D map of the simulation environment. The computational complexity of the ray tracing algorithm increases with the increase in the number of reflections and diffractions.

C. Simulation Environment

The target is to study the propagation in a small cell environment, therefore a courtyard area of NTT DOCOMO R&D center in Japan is considered for simulation. The Google map view of the target area is shown in Fig. 1. A simplified three-dimensional model of a target building created with MATLAB is shown in Fig. 2**.** Outdoor simulations are performed in an open area of the courtyard, whereas indoor simulations are done in the building area.

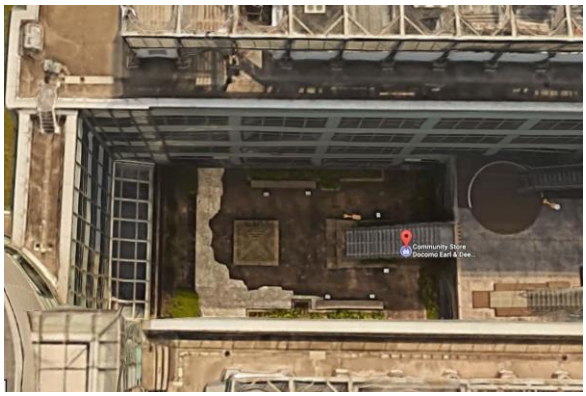

Fig. 1. Google map view of targeted courtyard area.

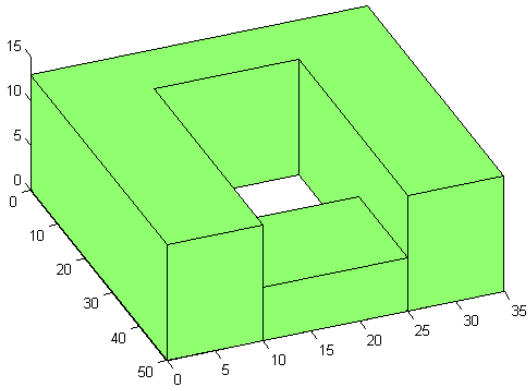

Fig. 2. Three-dimensional map of building with courtyard.

The simplified two-dimensional map of courtyard area generated through MATLAB is shown in Fig. 3. For both outdoor and indoor simulations, it is assumed that user is carrying a mobile phone at a height of 1.65 m and walking through the simulation routes. There are four outdoor (C1-C4),

and four indoor (C5-C8) simulation routes marked with red dots as shown in Fig. 3. All the outdoor paths are at the front of the transmitter antenna. Only the indoor path C5 lies behind the transmitter antenna. The exact location of the transmitter (TX) is marked with a blue spot, and the transmitter antenna is facing towards south. All the indoor and outdoor routes except C5 have a clear line-of-sight (LOS) with the transmitter. Two static points (one outdoor and one indoor) are marked as Pt1 and Pt2 are selected for power angular spectrum (PAS) analysis.

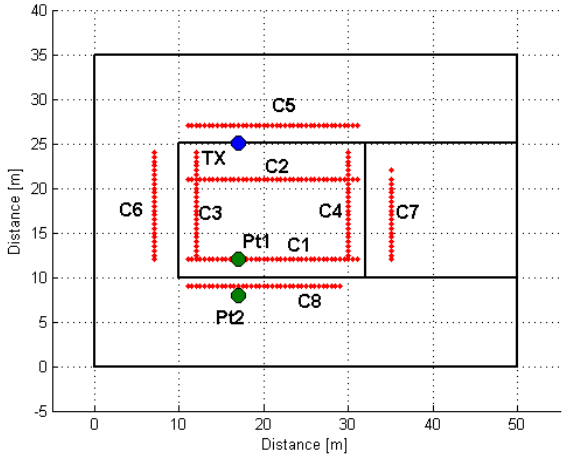

Fig. 3. Two-dimensional simulation area and the simulation routes.

For PAS simulations, a directive antenna with 14° HPBW in the horizontal domain and 10.5° HPBW in the vertical domain with 20 dBi maximum gain is utilized. It is assumed that a directive antenna on a receiver side at a height of 1.65 m is rotated by 360° in the azimuth plane with a step size of 5°. The general system simulation parameters are summarized in Table I.

Table I. General system simulation parameters for route simulations.

Parameters	**Unit**	**Value**
Frequency	GHz	15/28/60
Single carrier component (CC) bandwidth	MHz	100
System bandwidth (4 CCs)	MHz	400
Transmission power per CC	dBm	27.3
Total transmission power	dBm	33.32
Transmitter height	m	4
Antenna downtilt	°	2.3
MS height	m	1.65
Reflections		3
Diffractions		1
Diffuse scattering		Enabled

III. Simulation Results and Discussions

Fig. 4 shows the received signal strength in dBm for four outdoor and four indoor simulation routes. Fig. 4(a), Fig. 4(b) and Fig. 4(c) shows the received signal strength along the paths at 15 GHz, 28 GHz and 60 GHz, respectively. It can be seen that both C1 and C2 are in the main lobe of the transmitter. However, maximum signal levels are achieved along simulation path C1, whereas path C2 is nearer to the transmitter and that is due to the low value of downtilt. The measurement results in reference [11] also show similar trend. The maximum signal level of around -25 dBm is achieved at 15 GHz in the main lobe direction on path C1. It is hard to find the difference in received signal levels between the paths C3 and C4. The mean received signal level of all considered paths at 15 GHz, 28 GHz and 60 GHz are presented in Table II.

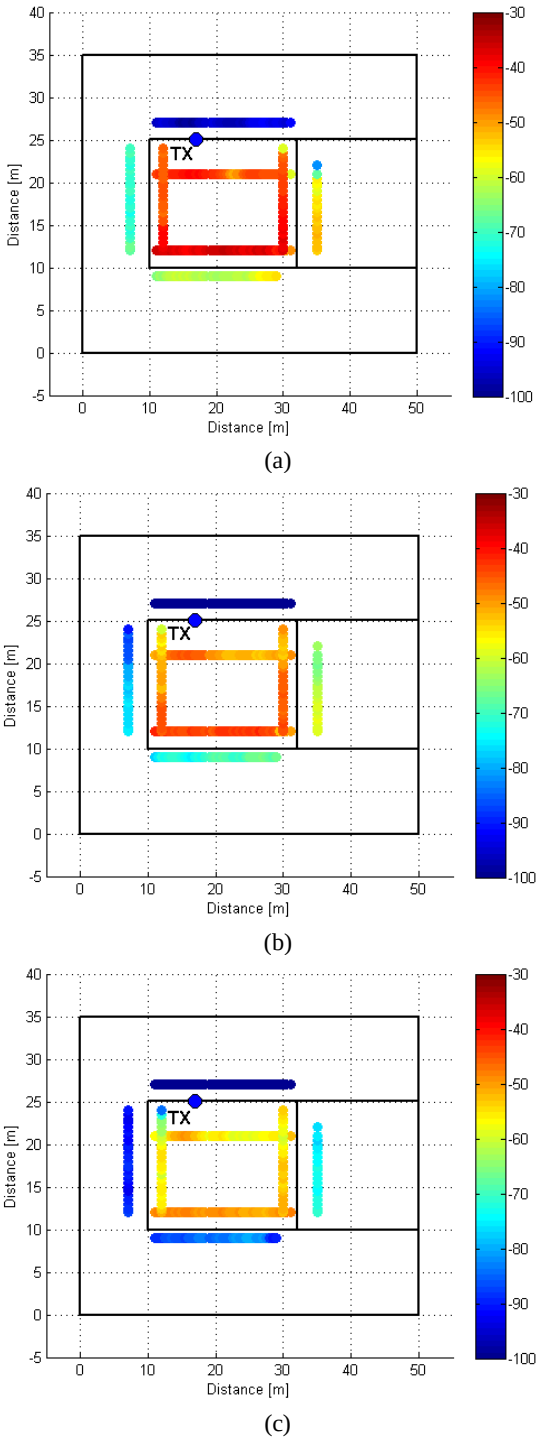

Fig. 4. Heat map of the received signal strength: (a) 15 GHz, (b) 28 GHz, and (c) 60 GHz.

Table II. Mean received signal strength level.

Simulation route	Mean RX level (dBm)		
	15 GHz	28 GHz	60 GHz
C1	-38.04	-44.11	-49.41
C2	-43.95	-49.40	-55.23
C3	-43.72	-50.17	-59.23
C4	-42.25	-47.85	-54.40
C5	-95.93	-121.45	-178.84
C6	-70.50	-80.29	-90.61
C7	-56.27	61.80	-73.77
C8	-60.82	-70.31	-84.64

It is found out that in outdoor cases, the mean difference of the received signal strength level between 15 GHz and 28 GHz is around 5-6 dB, and again there is a difference of around 8 dB between the received signal strength level of 28 GHz and 60 GHz. It shows that in outdoor small cell environment such a large transition between the frequencies does not make a large impact on the received signal levels. However, the signal propagation in an indoor environment has more impact of frequency transition. It can be seen in Table II that the building penetration loss is much higher at higher frequencies and that makes the received signal strength level quite low at higher frequencies in indoor environment.

Received signal levels are extremely low for path C5 as it was in the back lobe of the TX antenna, and the antenna was mounted on the wall. Path C6 is near the transmitter compared with path C7. Due to low antenna downtilt angle, the mean received signal strength level of path C7 is better than path C6, and this is the case in the measurement results provided for these two paths in reference [11]. It shows that simulation results provided in this paper are in a close relationship with the measurement results provided at reference [11]. It is also learned from the simulation results that an adequate indoor service can be provisioned at 15 GHz and 28 GHz. However, it is challenging to provide service to indoor user at 60 GHz using an outdoor base station even in such a small cell environment.

Fig. 5 show the normalized power angular spectrum of static location points Pt1 and Pt2. It can be clearly seen that the strongest LOS path is coming at the receiver point end North (90°) direction, and other strong reflected paths from three nearby sidewalls are evident to the outdoor location, i.e. Pt1. The strongest reflected path is around 10 dB lower in comparison with the LOS path. As Pt1 is located quite close to a wall, therefore a strong reflected multipath component is arriving from South direction i.e. -90°. Similarly, the major LOS, the reflected and diffracted paths, are the same at 28 GHz and 60 GHz. However, there are more scattering components in higher frequency and that makes the PAS smoother at 28 GHz and 60 GHz compared with 15 GHz.

Fig. 6 shows the power delay profile of Pt1 and Pt2 at 15 GHz. Both static points are located quite close to each other therefore an almost similar PDP is obtained for both points. A large number of multipath components show the multipath richness of environment. The courtyard is a small place therefore there is a small delay between the arrival of paths. An almost similar PDP is obtained for 28 GHz and 60 GHz. The mean delay spread for Pt1 and Pt2 are 118 ns and 103 ns, respectively.

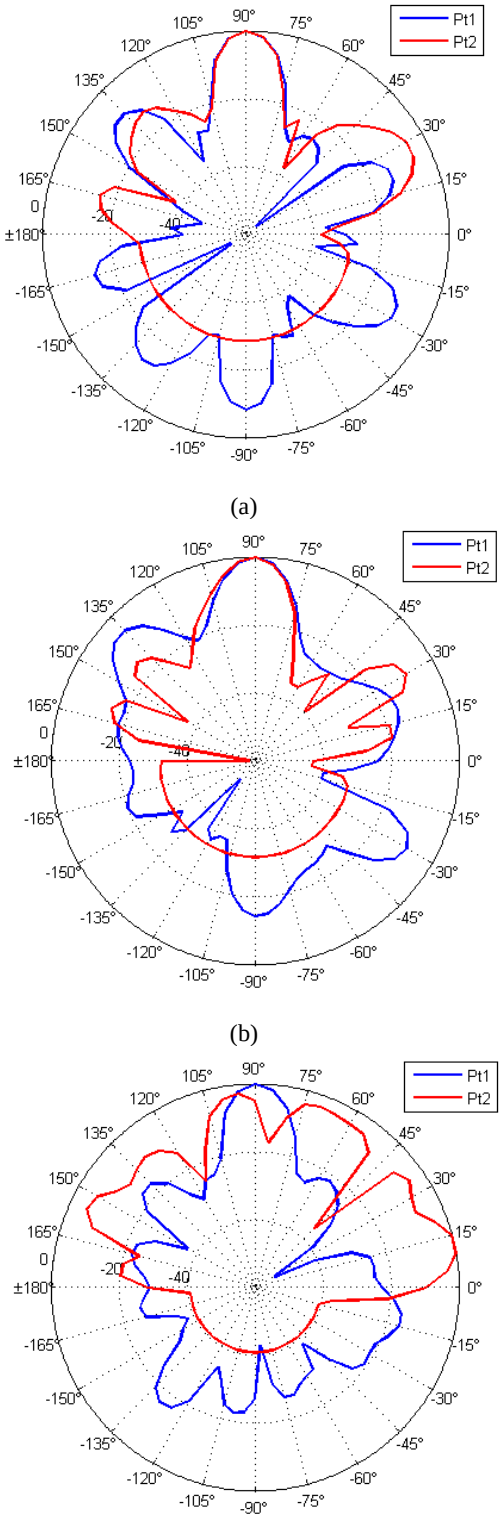

(a)

(b)

(c)

Fig. 5. Power angular spectrum at locations Pt1 and Pt2 at (a) 15 GHz, (b) 28 GHz, and (c) 60 GHz.

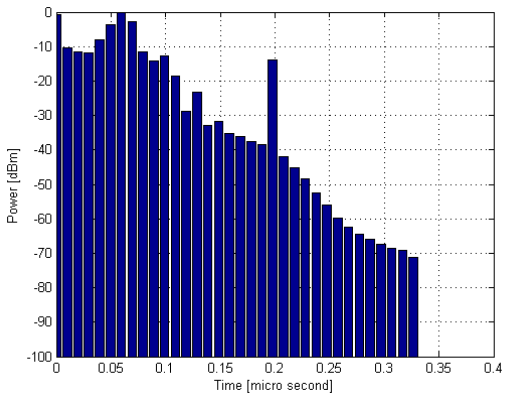

(a)

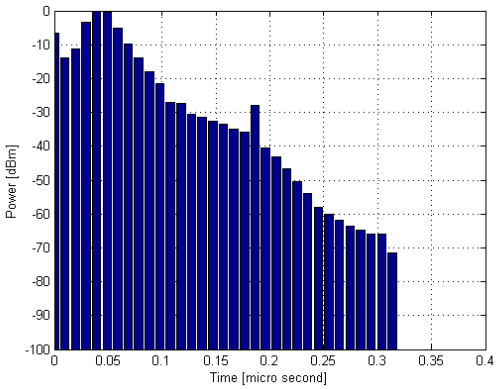

(b)

Fig. 6. Power delay profile at 15 GHz in (a) Pt1, and (b) Pt2.

IV. Conclusions

This paper has analyzed the propagation characteristics of an indoor and outdoor user at higher frequencies other than conventional frequency bands in a courtyard environment. The study was carried out by doing 3D ray tracing simulations. It is learned from simulation results that in small cell environment the mean difference of received signal level between 15 GHz and 28 GHz is around 5-6 dB, and a difference of around 8 dB between the received signal strength level at 28 GHz and 60 GHz. However, the signal starts to attenuate quickly in an indoor environment at higher frequencies due to higher building penetration loss and wall loss. Despite higher penetration loss, adequate indoor service can be provisioned at 15 GHz and 28 GHz. However, indoor service provision becomes challenging at 60 GHz. Results of power angular spectrum show that courtyard is a multipath rich environment, and the impact of scattering becomes more vigilant at higher frequencies. Acquired results show the potential of using higher frequency bands in a small cell environment.

Acknowledgment

The authors would like to thank European Communications Engineering (ECE) Ltd for supporting this research work.

References

[1] 3GPP, “Release 15”.

[2] Huawei Technologies, “5G: A Technology Vision”, White Paper, 2013.

[3] E. Dahlman, G. Mildh, S. Parkvall, J. Peisa, J. Sachs, Y. Selén, ”5G radio access,” Ericsson Review, vol. 91, no. 6, pp. 42–48, 2014.

[4] NTT DoCoMo, Inc, “5G Radio Access: Requirements, Concept and Technologies,” White Paper, 2014.

[5] T. S. Rappaport, J. N. Murdock and F. Gutierrez, “State of the art in 60 GHz integrated circuits & systems for wireless communications”, Proc. IEEE, vol. 99, pp. 1390-1436, 2011.

[6] W. Roh *et al.*, "Millimeter-wave beamforming as an enabling technology for 5G cellular communications: theoretical feasibility and prototype results," in IEEE Communications Magazine, vol. 52, no. 2, pp. 106-113, February 2014.

[7] S. G. Larew, T. A. Thomas, M. Cudak, A. Ghosh, “Air Interface Design and Ray Tracing Study for 5G Millimeter Wave Communications” in Proc. IEEE Globecom 2013, Atlanta, USA, 9-13 Dec, 2013.

[8] H. Zhao et al., “28 GHz Millimeter Wave Cellular Communication Measurements for Reflection and Penetration Loss in and Around Buildings in New York City,” IEEE ICC’13, June 2013, pp. 516–67.

[9] J. N. Murdock, E. Ben-Dor, Y. Qiao, J. I. Tamir and T. S. Rappaport, "A 38 GHz cellular outage study for an urban outdoor campus environment," 2012 IEEE Wireless Communications and Networking Conference (WCNC), Shanghai, 2012, pp. 3085-3090.

[10] Y. Inoue et al., "Field Experimental Trials for 5G Mobile Communication System Using 70 GHz-Band," 2017 IEEE Wireless Communications and Networking Conference Workshops (WCNCW), San Francisco, CA, 2017, pp. 1-6.

[11] K. Tateishi *et al.*, “Field experiments on 5G radio access using 15-GHz band in outdoor small cell environment,” Personal, Indoor, and Mobile Radio Communications (PIMRC), 2015 IEEE 26th Annual International Symposium on, Hong Kong, 2015, pp. 851-855.

[12] F. Fuschini, H. El-Sallabi, V. Degli-Esposti, L. Vuokko, D. Guiducci and P. Vainikainen, “Analysis of Multipath Propagation in Urban Environment Through Multidimensional Measurements and Advanced Ray Tracing Simulation,” in IEEE Transactions on Antennas and Propagation, vol. 56, no. 3, pp. 848-857, March 2008.

[13] D. N. Schettino, F. J. S. Moreira and C. G. Rego, “Efficient Ray Tracing for Radio Channel Characterization of Urban Scenarios," in 12th Biennial IEEE Conference on Electromagnetic Field Computation, Miami, FL, 2006, pp. 267-267.

[14] J.-E. Berg, “A Recursive Method for Street Microcell Pathloss Calculations”, Sixth IEEE International Symposium on Personal, Indoor and Mobile Radio Communications, PIMRC’95, Wireless: Merging onto the Information Superhighway. Vol. 1, 1995.

[15] X. Li, “Efficient Ray Tracing Simulation”, Master’s thesis at LUND University, 2014.

[16] M. U. Sheikh, K. Hiltunen and J. Lempiäinen, "Angular wall loss model and Extended Building Penetration model for out-door to indoor propagation," 2017 13th International Wireless Communications and Mobile Computing Conference (IWCMC), Valencia, 2017, pp. 1291-1296.